Numerical design of parallel multiresolution filter banks for image coding applications

Ashok Popat,† Wei Li, and Murat Kunt

Signal Processing Laboratory, Swiss Federal Institute of Technology
1015 Lausanne, Switzerland

ABSTRACT

A numerical technique is described for designing multiresolution, maximally decimated, parallel-structured, one-dimensional filter banks. The filter banks have properties which make them well suited to image subband coding applications. In particular, they provide nearly perfect reconstruction, are nearly orthogonal, provide joint localization in the spatial and spatial-frequency domains, and allow no leakage of DC into higher subbands. This paper describes the technique and presents a design example.

1. INTRODUCTION

In recent years, the idea of using linear transforms (including filter banks) that localize jointly in the original and transformed domains has gained popularity among researchers in the image coding community. From the standpoint of image coding, the attractiveness of such transforms lies in their ability to exploit both the spatial and spectral nonuniformity of energy distribution in an image in achieving energy compaction.

Another concept which has recently gained popularity among researchers is that of multiresolution transformation, wherein different spatial resolution scales are employed in carrying out the analysis and synthesis for each spectral component (subband), allowing the tradeoff between spatial and spectral resolution to be made differently for each one. Multiresolution transforms are well suited to image coding applications, where it is generally advantageous to employ smaller spatial regions of support when analyzing/synthesizing higher frequency subbands, and larger regions of support when analyzing/synthesizing lower frequency subbands. The advantage comes about because the high-frequency energy in images is typically due to phenomena of short spatial extent, such as edges, while the low-frequency energy comes from larger, more homogeneous regions.

Though much has been written about some of the mathematical questions surrounding multiresolution transforms, comparatively little published work addresses the practical problem of designing suitable transforms for real-world image coding applications. Moreover, much of the theory is concerned with the issue of strict invertibility of the transformation (i.e., mathematically perfect reconstruction).[1,2] In the authors' view, perfect reconstruction is a desirable but not essential property in many image coding applications. What is more important is that the analysis/synthesis process not be the source of appreciable degradation of the decoded image.

This paper describes a simple, reliable, and flexible numerical technique for designing jointly localizing multiresolution transforms, in the form of maximally decimated parallel-structured filter banks. Elements of the technique are based on previous work,[3,4] while the multiresolution and joint localization aspects are new. In contrast to many other design approaches, neither the fidelity of reconstruction nor the cancellation of aliasing derives from the structure of the filter bank. Instead, a fairly general structure is maintained, and a compound error criterion is formulated to represent the desired characteristics. This error criterion is minimized with respect to the individual filter coefficients via a gradient-based algorithm. A disadvantage of the approach is that a fast algorithm for implementation may not be found for a particular filter bank because of the lack of structure. An advantage is that the lack of structure provides flexibility: the filter bank can have an arbitrary number of bands, unequal bandwidths and sampling factors, and unequal regions of support for the filters.

---

† Ashok Popat is currently with PictureTel Corporation, One Corporation Way, Peabody, MA 01960. In September 1991, he will join the MIT Media Laboratory, Cambridge, MA 02139.

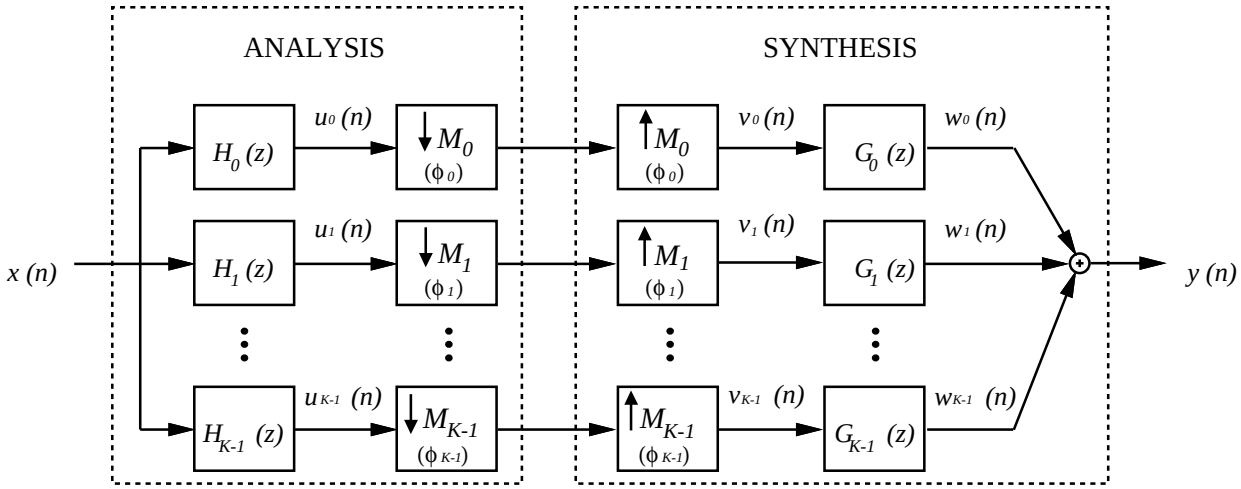

Figure 1: A parallel-structured filter bank with integer subsampling and upsampling.

The technique presented here can be used to design filter banks tailored to a wide variety of applications, and can be extended to several dimensions, provided that computational resources are sufficient. Here, consideration is restricted to the problem of designing one-dimensional filter banks for the purpose of separable subband analysis/synthesis of images. These filter banks, in addition to having the desirable joint localization and multiresolution properties, have other properties that make them suitable for use in image subband coding: (1) they provide nearly perfect reconstruction, (2) they are nearly orthogonal, and (3) the DC component is strictly confined to lie entirely within the lowest frequency subband.

This paper is organized as follows. In Section 2, some useful notation is introduced, and the space-domain input-output relationship is derived for a general integer-sampled parallel-structured filter bank. Mention is also made of the connection between parallel-structured and tree-structured filter banks. Section 3 discusses localization, and proposes a criterion by which to gauge it in both the spatial and spectral domains. In Section 4, design constraints suggested by the image coding application are discussed, and a compound error criterion for optimizing the filter bank is described. In Section 5, the optimization procedure is discussed, and a design example is presented.

2. PARALLEL-STRUCTURED ANALYSIS/SYNTHESIS FILTER BANK

Consider the one-dimensional analysis/synthesis system shown in Figure 1. In the analysis portion, the input signal $x(n)$ is first analyzed into K subband signals by a bank of parallel FIR filters $\{H_0(z), \ldots, H_{K-1}(z)\}$. Since the filter bank will be used for separable subband analysis/synthesis, the sequence index n corresponds to either the horizontal or vertical spatial dimension. After filtering, each subband signal $u_k(n)$ is subsampled by an integer factor M_k, where the sampling lattice is shifted to include the sample indexed by ϕ_k. It is assumed that the sampling phase ϕ_k is a parameter in the range $0, \ldots, M_k - 1$. The subsampled subband signals constitute the output of the analysis portion of the system. In a typical coding application, these signals would be encoded, transmitted, and decoded before synthesizing. Here, we assume there is no such intermediate processing. In the synthesis portion of the system, the subsampled subband signals are upsampled by zero-insertion to their original rates and lattice positions, forming the signals $v_0(n), \ldots, v_{K-1}(n)$. Each $v_k(n)$ is then filtered using an FIR interpolation filter $G_k(z)$, forming the signals $w_0(n), \ldots, w_{K-1}(n)$. These interpolated subband signals are then summed together to yield the final output $y(n)$.

Let $h_k(n)$ denote the impulse response of the k^{th} analysis filter, and let $R_{h,k}$ denote the region of support of that filter. Similarly, let $g_k(n)$ and $R_{g,k}$ be the impulse response and region of support, respectively, of the k^{th} synthesis

filter. Thus,

$$H_k(z) = \sum_{n \in R_{h,k}} h_k(n) z^{-n} \qquad \text{and} \qquad G_k(z) = \sum_{n \in R_{g,k}} g_k(n) z^{-n}.$$

The input-output relationship of the analysis/synthesis filter bank is obtained simply by tracing through the signal paths from left to right, beginning with the signals $u_0(n), \ldots, u_{K-1}(n)$, which are obtained immediately by convolution:

$$u_k(n) = \sum_{j \in R_{h,k}} h_k(j) x(n-j). \tag{1}$$

To obtain $v_k(n)$, observe that the cascade of subsampling and upsampling by a factor M_k, with phase ϕ_k, is equivalent to setting all but every M_k^{th} sample to zero, in such a way that the sample indexed by ϕ_k is included among the unsuppressed samples. The relationship between $u_k(n)$ and $v_k(n)$ can thus be expressed as

$$v_k(n) = \begin{cases} u_k(n) & \text{if } n = \phi_k, \pm M_k + \phi_k, \pm 2M_k + \phi_k, \ldots; \\ 0 & \text{otherwise.} \end{cases} \tag{2}$$

Combining (1) and (2) yields

$$v_k(n) = \begin{cases} \sum_{j \in R_{h,k}} h_k(j) x(n-j) & \text{if } n = \phi_k, \pm M_k + \phi_k, \pm 2M_k + \phi_k, \ldots; \\ 0 & \text{otherwise.} \end{cases} \tag{3}$$

Next, each $v_k(n)$ is filtered using $G_k(z)$. The convolution of $v_k(n)$ with $g_k(z)$ can be expressed as

$$\begin{aligned} w_k(n) &= \sum_{i \in R_{g,k}} g_k(i) v(n-i) \\ &= \sum_{i \in \mathcal{I}_{n,\phi_k}} \sum_{j \in R_{h,k}} g_k(i) h_k(j) x(n-i-j), \end{aligned} \tag{4}$$

where $\mathcal{I}_{n,\phi_k}$ is defined as

$$\mathcal{I}_{n,\phi_k} = \left\{ i : i \in R_{g,k} \text{ and } (n-i) \in \{\phi_k, \pm M_k + \phi_k, \pm 2M_k + \phi_k, \ldots\} \right\}.$$

The complete space-domain expression for the input-output relationship is obtained by summing together the interpolated subband signals $w_0(n), \ldots, w_{K-1}(n)$:

$$y(n) = \sum_{k=0}^{K-1} \sum_{i \in \mathcal{I}_{n,\phi_k}} \sum_{j \in R_{h,k}} g_k(i) h_k(j) x(n-i-j). \tag{5}$$

Note that the right hand side of (5) is similar to the expression that would have been obtained had there been no subsampling and upsampling; the difference is that the second summation is carried out over $i \in \mathcal{I}_{n,\phi_k}$ (where $\mathcal{I}_{n,\phi_k} \subset R_{g,k}$) instead of simply over $i \in R_{g,k}$.

Two useful observations can be made about the filter bank as characterized by the input-output relationship (5). First, it is clear that the overall system is linear. Second, the overall system is periodically shift-varying, where the period is the least common multiple of the M_k's. Let P denote this period; that is, let

$$P = \text{LCM } \{M_0, \ldots, M_{K-1}\}.$$

Because the filter bank is linear and periodically shift varying, it can be characterized by its individual responses to P unit-sample sequences (impulses), each shifted by a different amount in the range $0, \ldots, P-1$. Let $t_p(n)$ be

defined as the response of the filter bank to the input $\delta(n-p)$, shifted to lie as if the impulse had occurred at zero. That is, define $t_p(n)$ as

$$\begin{aligned} t_p(n) &= y(n+p)\big|_{x(n)=\delta(n-p)} \\ &= \sum_{k=0}^{K-1} \sum_{i \in \mathcal{I}_{n+p,\phi_k}} g_k(i) h_k(n-i), \end{aligned} \tag{6}$$

for $p = 0, 1, \ldots, P-1$, where

$$\mathcal{I}_{n+p,\phi_k} = \left\{ i : i \in R_{g,k} \text{ and } (n+p-i) \in \{\phi_k, \pm M_k + \phi_k, \pm 2M_k + \phi_k, \ldots\} \right\}.$$

Note that, if the filter bank is designed so that $t_p(n)$ is independent of p, then the filter bank will be shift-invariant, which implies that it will be alias-free (since complex exponentials are eigenfunctions of linear shift-invariant systems). If, in addition, $t_p(n) = \delta(n-D)$ for some appropriate constant shift D, then the output will be a perfect replica of the input; i.e., the filter bank will provide perfect reconstruction. In Section 4, this observation will be used in formulating the compound error criterion for filter bank design.

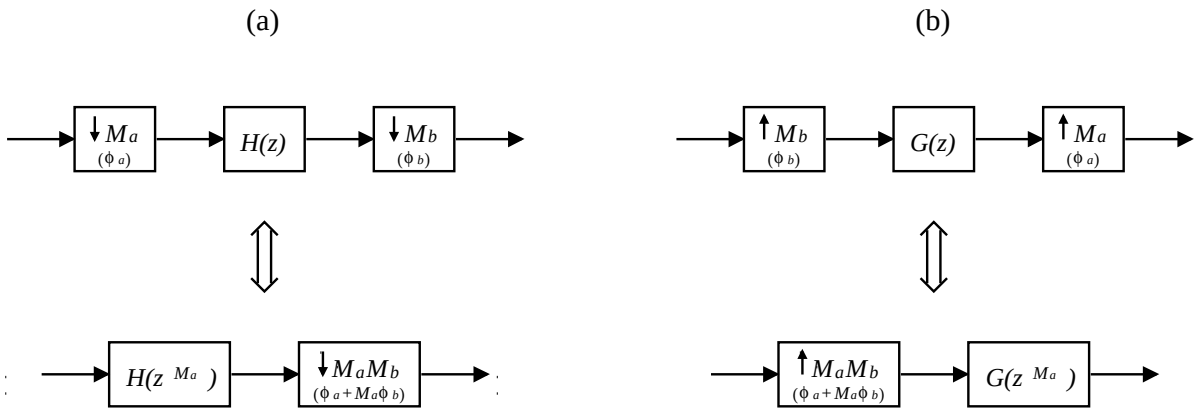

Figure 2: Identity relationships that can be used to transform an arbitrary tree-structured filter bank into an equivalent parallel-structured one. Identity (a) is applied as necessary to the analysis portion, while (b) is applied to the synthesis portion. Adapted from Vaidyanathan,[5] to take sampling phase into account.

While the foregoing analysis is valid for arbitrary values of $M_0, \ldots, M_{K-1}$, not all choices for these sampling factors will make possible perfect reconstruction (or nearly perfect reconstruction). In the present study, consideration is restricted to values of $M_0, \ldots, M_{K-1}$ for which the authors know that perfect reconstruction is possible when FIR filters are used. In particular, consideration is restricted to those values of $M_0, \ldots, M_{K-1}$ for which there exists a tree-structured filter bank, composed of uniform-band analysis/synthesis elements, having the same effective sampling factors at the leaves of the tree. Henceforth, a tree-structured filter bank composed of uniform-band analysis/synthesis elements will be termed a *uniform-element tree*. Such a tree can always be expressed in parallel form, by applying the identity relationships shown in Figure 2. If each uniform analysis/synthesis component in the tree provides perfect reconstruction, then the whole tree and its parallel equivalent will likewise provide perfect reconstruction. Uniform perfect-reconstruction FIR filter banks exist for an arbitrary number of bands; a trivial example is the uniform analysis/synthesis bank where each filter is the identity filter (i.e., no filtering is done at all), and where the sampling phase is different for every subband. A less trivial example is the filter-bank realization of

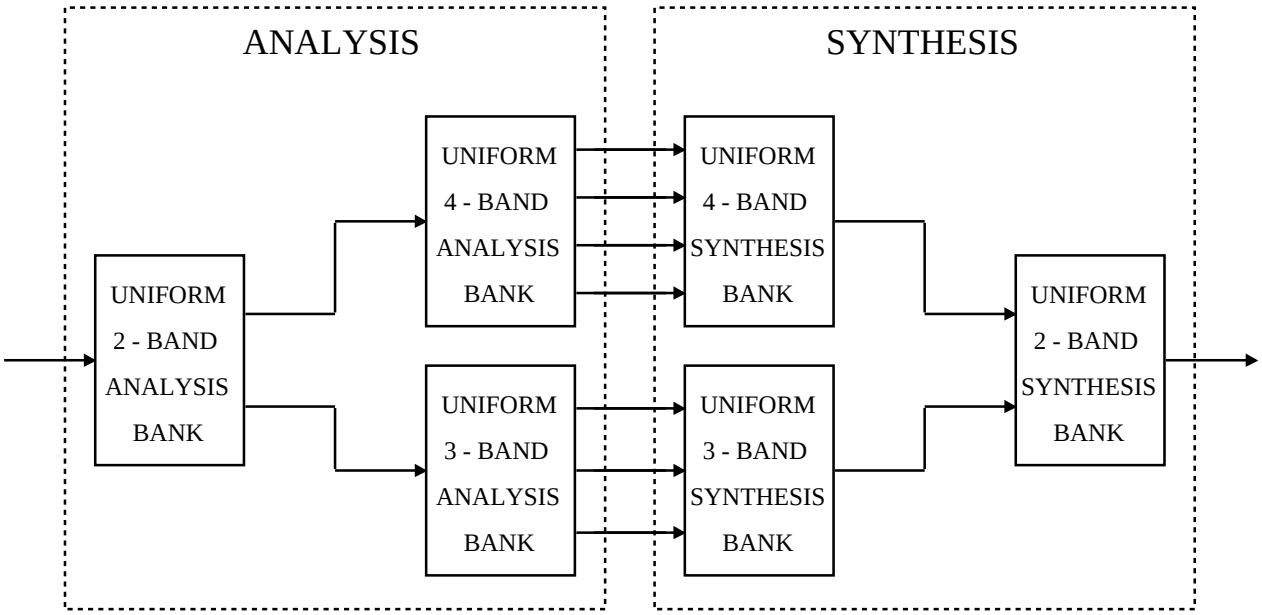

Figure 3: An example of a tree-structured filter bank, comprised of uniform 2-, 3-, and 4-band analysis/synthesis filter banks. By applying the identities of Figure 2, an equivalent 7-band parallel-structured filter bank can be obtained. The equivalent sampling factors are $\{8, 8, 8, 8, 6, 6, 6\}$.

the discrete cosine transform (DCT). A parallel-structured perfect-reconstruction filter bank corresponding to the former will be termed *impulse-derived*, while one corresponding to the latter will be termed *DCT-derived*.

The tree-derivable restriction on the sampling factors is imposed for two reasons. First, a uniform-element tree can be used to generate a convenient perfect-reconstruction initial guess for the design procedure. Second, the authors have found through experimentation that if the sampling factors are not tree derivable, then the reconstruction error can be made small only by making the filters very long, contrary to the joint localization objective.

This restriction on the sampling factors can be made clearer with an example. Suppose the sampling factors in a 7-band parallel-structured filter bank are chosen to be $\{8, 8, 8, 8, 6, 6, 6\}$. Since there exists a uniform-element tree having equivalent sampling factors at its leaves (an example is shown in Figure 3), this particular set of sampling factors is considered admissible in the present study.

Note that the stated condition on the sampling factors is more restrictive than the condition that the degrees of freedom in the input signal not be reduced, i.e., $\sum_k 1/M_k \geq 1$. For example, a 3-band filter bank with sampling factors $\{2, 3, 6\}$ preserves degrees of freedom, but is inadmissible in the present study because no uniform-element tree has equivalent sampling factors at its leaves.

While any tree-structured filter bank can be expressed in a parallel form, not every parallel-structured filter bank can be expressed as a uniform-element tree. In this sense, the parallel structure is more general than the uniform-element tree structure, and may afford greater freedom in optimizing the spatial and spectral localization characteristics of the filter bank. This simple observation provided the principal motivation for the present investigation.

3. SPATIAL AND SPECTRAL LOCALIZATION

A filter is said to be localized in space if the energy in its impulse response is concentrated within a sufficiently small

spatial neighborhood. Similarly, a filter is said to be localized in frequency if the area under its magnitude response curve is concentrated in a sufficiently small segment of the frequency axis. If a filter is localized in both domains, then it is said to be *jointly localized*. It is well known that a filter cannot be arbitrarily local in both domains; to achieve a certain frequency resolution, a sufficiently long space window must be used, while a short space window implies coarse frequency resolution.

The definition of joint localization given above is somewhat vague, and it is possible to formulate several different explicit measures for joint localization, each of which is consistent with it. In general, in the absence of other constraints, different explicit measures of joint localization will lead to different "optimally localizing" filters. However, once the constraints on the filter bank suggested by the image coding application are imposed (i.e., near orthogonality, nearly perfect reconstruction, and strict confinement of DC to the lowest-frequency subband), the individual filters may no longer bear a strong resemblance to the unconstrained "optimally localizing" filters. The aim of this section is to propose a joint-localization criterion that is useful in the filter bank design problem, in the sense that using it in a constrained minimization results in filters that have jointly localizing properties in the vague sense mentioned above, while simultaneously meeting the other design objectives suggested by the image coding application.

In the remainder of this section, consideration is restricted to the localization properties of a single filter $H(z)$, having impulse response $h(n)$ and region of support R_h. In Section 4, it will be seen how the criterion proposed here can be used in defining an objective function for optimization of the entire filter bank.

Discussion begins with the classic work of Gabor.[6] Working with continuous-space signals and systems, he proposed a certain criterion for joint localization, and showed that the filters which optimize it have impulse responses that are sinusoids weighted by a Gaussian envelope. For a continuous-space filter with real impulse response $h_c(t)$ and Fourier transform $H(f)$, Gabor's criterion can be written

$$G = \frac{1}{E_c^2}\Big[\int_{-\infty}^{\infty}(t-t_c)^2 h_c^2(t)dt\Big]\Big[\int_{-\infty}^{\infty}(f-f_c)^2|H(f)|^2 df\Big], \tag{7}$$

where $E_c = \int_{-\infty}^{\infty} h_c^2(t)dt$, and where t_c and f_c are given constants. In considering the discrete-space localization problem, it is natural to question whether sampled versions of Gabor's jointly localizing continuous-space functions can be used as the impulse responses in a filter bank for image coding. Daugman investigated this possibility, using sampled two-dimensional Gabor functions for the analysis filters.[7] Unfortunately, the corresponding synthesis filters are poorly behaved, and the resulting filter bank is strongly nonorthogonal.[8]

An alternative would be to attempt to apply Gabor's criterion in an optimization procedure, while subjecting the filters to the given application-specific constraints. For this, a discrete-space measure analagous to Gabor's is required. Upon cursory examination, it would seem that a natural choice would be the expression obtained by replacing the first integral in (7) with a summation, and by adjusting the second integral for the periodic spectrum. The resulting criterion would be

$$G_d = \frac{1}{E^2}\Big[\sum_{n\in R_h}(n-n_c)^2 h^2(n)\Big]\Big[\int_0^{\pi}(\omega-\omega_c)^2|H(\omega)|^2 d\omega\Big], \tag{8}$$

where $E = \sum_{n\in R_h} h^2(n)$, and where n_c and w_c are given constants. Unfortunately, this measure turns out not to be very useful, since it is minimized by $h(n) = \delta(n-n_c)$ — which provides no spectral localization at all.

The problem of joint localization in the discrete case has been considered extensively by Slepian.[9] He proposed the following localization measures:

$$S_n = \frac{1}{E}\sum_{n=n_1}^{n_2} h^2(n), \tag{9}$$

and

$$S_\omega = \frac{1}{E}\int_{W_1}^{W_2}|H(\omega)|^2 d\omega, \tag{10}$$

where E is defined as above, and where n_1, n_2, W_1, and W_2 are parameters. Slepian derived the set of possible joint values of S_n and S_ω, paying particular attention to the cases where one of the two measures is constrained to be zero. It would seem that Slepian's measures are well suited to the present application, since the ideal band edges are known, and since consideration is restricted to FIR filters. However, a potential disadvantage of using Slepian's spatial measure is that the region of support for each filter would be a critical parameter, and it is not clear how this parameter should be selected. For this reason, the use of Slepian's measures was not explored further in the present study. Instead, it is suggested as a topic for further research.

As an alternative, the following *ad hoc* additive joint localization measure is proposed:

$$E_{n,\omega} = \alpha_n E_n + \alpha_\omega E_\omega, \tag{11}$$

where

$$E_n = \frac{1}{E}\Big[\sum_{n \in R_h} (n - n_c)^2 h^2(n)\Big]; \tag{12}$$

$$E_\omega = \frac{1}{E}\Big[\int_0^\pi (\omega - \omega_c)^2 |H(\omega)|^2 d\omega\Big], \tag{13}$$

and where E is defined as above, and α_n and α_ω are positive weighting constants. To facilitate computation, the integral in (13) can be evaluated explicitly to obtain the following analytic expression for E_ω:

$$E_\omega = \frac{\pi^2}{3} - \pi\omega_c + \omega_c^2 + \frac{4}{E}\sum_{n=\min R_h}^{\max R_h - 1}\sum_{m=n+1}^{\max R_h} h(n)h(m)\frac{(1-\omega_c/\pi)(-1)^{n-m} + \omega_c/\pi}{(n-m)^2}. \tag{14}$$

Note that $E_{n,\omega}$ resembles G_d, but employs a sum rather than a product of spatial and spectral localization terms.

This section concludes with an example that demonstrates the effectiveness of the proposed criterion in measuring joint spatial/spectral localization. Figure 4 illustrates the control that can be exercised over the spatial/spectral localization tradeoff for a bandpass filter centered at $\omega_c = 0.4\pi$ and $n_c = 0$, by numerically minimizing $E_{n,\omega}$ for different values of the ratio α_ω/α_n. To achieve the minimization, the optimization procedure described in the Appendix was used, beginning with $\delta(n)$ as the initial guess. The filter was constrained to have zero phase and unit energy via the penalty function method.[10] Although this example demonstrates that the proposed criterion measures joint localization, its ultimate justification in the present study lies its usefulness in designing filter banks with desirable properties for image coding applications. This usefulness will be demonstrated by the design example given in Section 5.

4. A COMPOUND ERROR CRITERION FOR OPTIMIZATION

This section describes a compound error criterion for the design of a maximally decimated, parallel-structured, multiresolution filter bank through numerical optimization. The error criterion reflects the objectives of nearly perfect reconstruction, spatial/spectral localization, and strict confinement of DC to the lowest subband. In addition, this section describes a simple constraint on optimization that results in near-orthogonality of the filter bank.

4.1 A measure of reconstruction error

As mentioned in Section 2, perfect reconstruction will occur when each of the P distinct impulse responses $t_p(n)$ is equal to a delayed delta function, $\delta(n - D)$, for some suitable value of delay D. This observation leads naturally to the following simple square-error expression for reconstruction error:

$$E_{\mathrm{R}} = \frac{1}{P}\sum_{n \in R_t}\sum_{p=0}^{P-1}\big[t_p(n) - \delta(n - D)\big]^2, \tag{15}$$

where $t_p(n)$ is defined as in Section 2, D is a parameter, and R_t is the set of indices n for which $t_p(n)$ is potentially nonzero. For convenience, D is always chosen to be zero in the present study (the filters are not required to be causal).

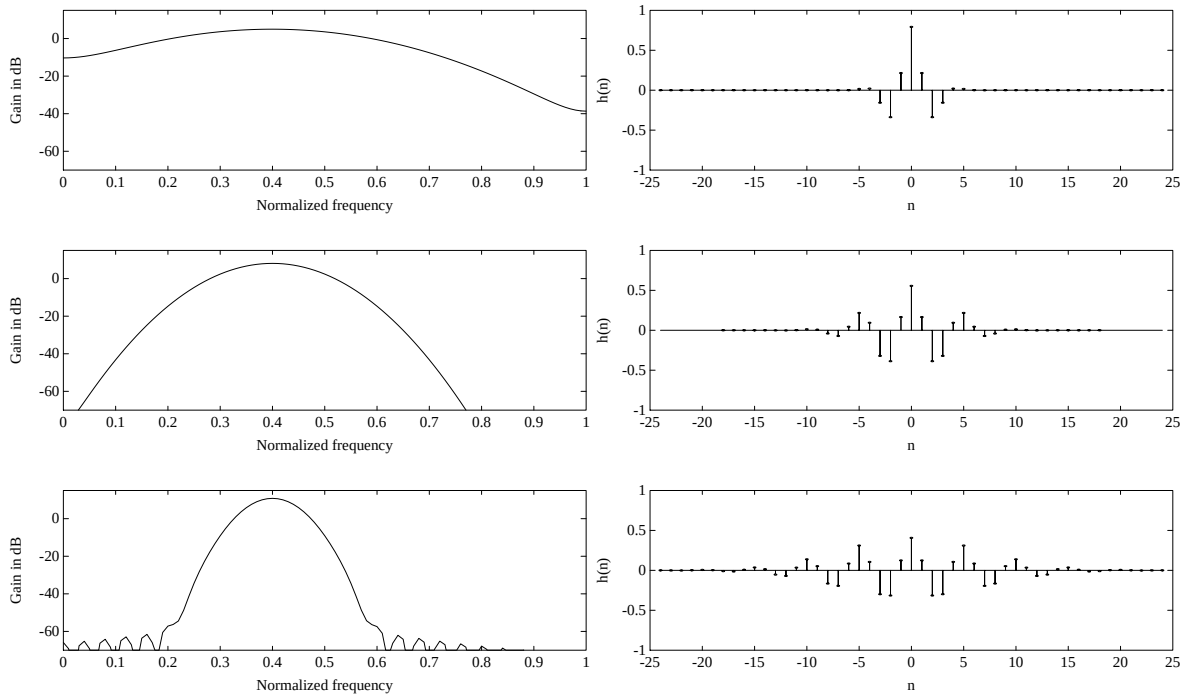

Figure 4: Example of the design of a bandpass filter $H(z)$ centered at $\omega_c = 0.4\pi$ and $n_c = 0$, via numerical minimization of $E_{n,\omega}$ as given by (11). The region of support is $R_h = \{-24, \ldots, 24\}$. The minimization was carried out subject to the constraints $\sum_n h^2(n) = 1$ and $h(n) = h(-n)$. The initial guess in each case was $h(n) = \delta(n)$, and the choices of the ratio α_ω/α_n for the three cases were: (top) 10, (middle) 100, and (bottom) 10,000.

4.2 Near-orthogonality

Here, the term *orthogonality* is used in the sense described by Simoncelli and Adelson.[8] The analysis and synthesis portions of the filter bank are linear, and hence have matrix representations for finite-duration signals. Suppose the samples of a very long but finite-duration input signal are grouped into a large column vector. The corresponding vector of subband samples can be obtained by premultiplying the vector by an analysis matrix. The rows of this matrix are simply shifted versions of the impulse responses of the analysis filters. The corresponding vector of output samples can then be obtained by premultiplying by another matrix, which has as its columns space-reversed and shifted versions of the synthesis filter impulse responses. If the impulse response of each synthesis filter is a space-reversed version of the impulse response of the corresponding analysis filter, then the matrices are transposes of each other. If, in addition, the filter bank provides perfect reconstruction, then the analysis and synthesis matrices are inverses of each other, so that the matrices are orthogonal. A filter bank for which the corresponding analysis and synthesis matrices are orthogonal is said to be orthogonal. Orthogonal transformations preserve length, and hence energy. In relation to subband coding, this property implies that (1) the total subband energy will equal the total input energy, and (2) the overall mean-square coding distortion will be the sum of the individual distortions incurred in coding each subband.

If the filter banks were to provide truly perfect reconstruction, then to obtain orthogonality it would be sufficient to constrain the impulse responses of the analysis and corresponding synthesis filters to be space-reversed versions of each other. By imposing this constraint in the near-perfect reconstruction case, near-orthogonality results. The space-reversal constraint can be written

$$h_k(n) = g_k(N - n), \tag{16}$$

for $k = 0, \ldots, K-1$ and $n \in R_{h,k}$, where N is a parameter, and $R_{g,k}$ is defined to be $\{i : (N-i) \in R_{h,k}\}$. For convenience, N is taken to be zero, so that the space-reversal constraint is

$$h_k(n) = g_k(-n). \tag{17}$$

Imposing the space-reversal constraint (17) provides two additional benefits besides ensuring near-orthogonality. First, the dimensionality of the optimization problem is cut in half. Second, experience has shown that without this constraint, the resulting filters occasionally have poorly behaved magnitude-frequency responses.

4.3 Joint localization

To measure joint localization, a separate $E_{n,\omega}$ is computed for each analysis filter, and their simple weighted sum is taken. The synthesis filters need not be considered because of the space-reversal constraint. The resulting joint localization criterion E_{L} can be written in the form

$$E_{\mathrm{L}} = \sum_{k=0}^{K-1} \left[\alpha_{n,k} E_{n,k} + \alpha_{\omega,k} E_{\omega,k}\right], \tag{18}$$

where

$$E_{n,k} = \frac{1}{E_k}\Big[\sum_{n \in R_{h,k}} (n - n_{c,k})^2 h_k^2(n)\Big]; \tag{19}$$

$$\begin{aligned} E_{\omega,k} &= \frac{1}{E_k}\Big[\int_0^{\pi} (\omega - \omega_{c,k})^2 |H_k(\omega)|^2 d\omega\Big] \\ &= \frac{\pi^2}{3} - \pi\omega_{c,k} + \omega_{c,k}^2 + \frac{4}{E} \sum_{n=\min R_{h,k}}^{\max R_{h,k}-1} \sum_{m=n+1}^{\max R_{h,k}} h_k(n) h_k(m) \frac{(1-\omega_{c,k}/\pi)(-1)^{n-m} + \omega_{c,k}/\pi}{(n-m)^2}, \end{aligned} \tag{20}$$

and where $E = \sum_{n \in R_{h,k}} h_k^2(n)$; $\omega_{c,k}$ and $\omega_{n,k}$ are spectral and spatial subband midpoints, respectively; and $\alpha_{n,k}$ and $\alpha_{\omega,k}$ are positive weighting parameters.

4.4 Strict confinement of DC

In image subband coding practice, it is important that the DC component not "leak" into higher subbands. Strict confinement of DC will occur when all of the analysis and synthesis filters, except the lowest-frequency ones, have zeroes at DC. Again, because of the space-reversal constraint, only the analysis filters need be considered. Accordingly, the following penalty function is defined:

$$E_{\mathrm{DC}} = \sum_{k=1}^{K-1} \Big[\sum_{n \in R_{h,k}} h_k(n)\Big]^2. \tag{21}$$

Since E_{DC} does not compete in any fundamental way with the other error terms, the penalty function method is an effective means of imposing the DC-confinement constraint.

4.5 A compound error criterion

The foregoing individual error terms can be combined in a weighted sum, to yield a single objective criterion for optimization of the filter bank. That criterion is

$$E_{\mathrm{total}} = \alpha_{\mathrm{R}} E_{\mathrm{R}} + \sum_{k=0}^{K-1} \left[\alpha_{n,k} E_{n,k} + \alpha_{\omega,k} E_{\omega,k}\right] + \alpha_{\mathrm{DC}} E_{\mathrm{DC}}. \tag{22}$$

The following section discusses numerical minimization of E_{total}.

5. OPTIMIZATION AND DESIGN EXAMPLE

The compound error criterion proposed in the previous section measures the degree to which the filter bank satisfies the design objectives of near-perfect reconstruction, joint localization, and strict confinement of DC to the lowest-frequency subband. The synthesis filter coefficients were removed as free variables from the problem, by imposing a space-reversal constraint (17). Thus, the filter bank design problem has become one of numerically minimizing E_{total} over the space of analysis filter coefficients.

It is easy to verify that the partial derivatives of E_{total} with respect to the analysis filter coefficients exist everywhere and are continuous. Moreover, analytical expressions for them are readily derivable. Consequently, E_{total} can be minimized via a gradient-based technique. Any of a number of well-known algorithms can be used to carry out the optimization. In the present study, the simple gradient-based algorithm described in the Appendix is used, primarily because of ease of implementation.

Before an optimization procedure can be applied, parameter values must be selected, and an initial guess chosen. Some of the parameter values are determined by the application; these include the number of bands, the sampling factors, and the regions of support of the filters.

Appropriate center frequencies can be determined directly from the sampling factors. Suitable values for $\omega_{c,0}$ and $\omega_{c,K-1}$ are 0 and π, respectively, while for the intermediate center frequencies, the centers of the ideal subbands can be used:

$$\omega_{c,k} = \pi\left[\frac{1}{2M_k} + \sum_{i=0}^{k-1} \frac{1}{M_i}\right]. \tag{23}$$

Suitable values for the weighting constants in (22) are determined empirically. The penalty functions E_{R} and E_{DC} should have large weights to minimize reconstruction error and leakage of DC, but large weights slow down the optimization. For this reason, it is suggested that the optimization be carried out in two phases. Small weights should be used for E_{R} and E_{DC} in the first stage, while large ones should be used in the second. A good rule-of-thumb is to select the weights $\{\alpha_{n,k}\}$ and $\{\alpha_{\omega,k}\}$ first to get the desired localization ratios, then to set α_{R} and α_{DC} each to be of roughly the same order of magnitude as the largest $\{\alpha_{\omega,k}\}$ for the initial phase of optimization. In the second phase, α_{R} and α_{DC} can be increased by two or three orders of magnitude so that the reconstruction error and DC leakage are minimized.

Experience has shown that the final result of optimization is relatively insensitive to the choice of initial guess. However, the number of iterations required for convergence of the optimization can be significantly reduced by judicious choice of an initial guess. A suitable initial guess can be obtained by converting a perfect-reconstruction uniform-element tree into a parallel structure, as discussed in Section 2. Both impulse-derived and DCT-derived initial guesses have been found to work well in all cases.

Figure 5 shows the frequency-magnitude response curves of the analysis filters in two design examples. In both cases, the sampling factors are $\{6, 6, 3, 3\}$, and the initial guess is impulse-derived. In the first, the spatial/spectral localization tradeoff is made equally for all subbands. In the second, the higher-frequency subbands have poorer spectral localization but better spatial localization than the lower-frequency subbands. The reconstruction error E_{R} is 2.68×10^{-7} for MULTI-4-A, and 1.09×10^{-7} for MULTI-4-B.

6. CONCLUSION

A numerical technique for designing multiresolution, maximally decimated, parallel-structured, one-dimensional filter banks has been presented. The resulting filter banks have properties which make them suitable for image subband coding applications. These properties include joint spatial/spectral localization, nearly perfect reconstruction, near-orthogonality, and strict confinement of DC to the lowest-frequency subband. The technique appears to be effective and reliable.

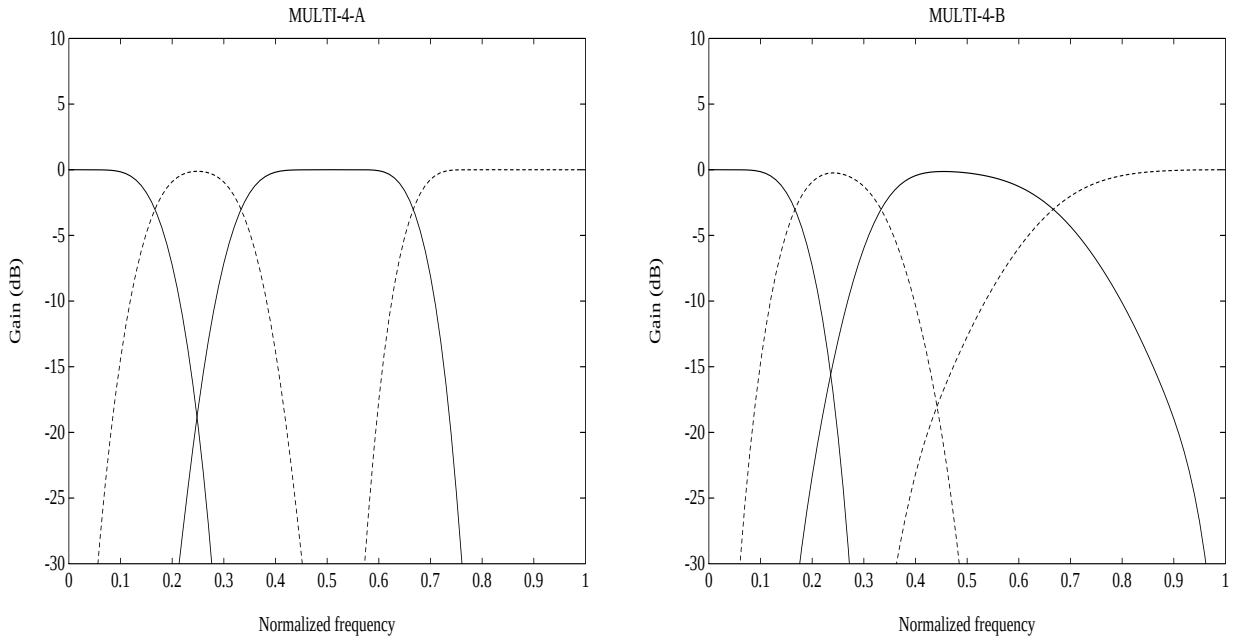

Figure 5: Frequency-magnitude response curves of analysis filters for two design examples. See Tables 1 and 2 for parameters and coefficient values. To equalize the passband gains in the graphs, a scaling factor of $1/\sqrt{M_k}$ has been applied to each $h_k(n)$. The reconstruction error E_{R} is 2.68×10^{-7} for MULTI-4-A, and 1.09×10^{-7} for MULTI-4-B.

APPENDIX: A SIMPLE OPTIMIZATION PROCEDURE

This appendix presents a simple procedure for finding a local minimum of a smooth, nonlinear, scalar-valued function of a vector.

Let $\langle \mathbf{u}, \mathbf{v} \rangle$ denote the Euclidean inner (dot) product of the n-dimensional vectors $\mathbf{u}$ and $\mathbf{v}$. Let $\|\mathbf{u}\|$ denote the Euclidean norm of an n-dimensional vector $\mathbf{u}$. Let $\{\mathbf{x}_k\}$, $k = 0, 1, \ldots$, be a sequence of n-dimensional vectors, let $x_{k\,i}$ denote the i^{th} component of $\mathbf{x}_k$, and let $F(\mathbf{x}_k)$ be a scalar-valued function of $\mathbf{x}_k$ for which the partial derivatives $\partial F(\mathbf{x}_k)/\partial x_{k\,i}, i = 1, \ldots, n$, are continuous and available in analytic form. The gradient of $F(\mathbf{x}_k)$, denoted $\nabla F(\mathbf{x}_k)$, is an n-dimensional vector function of $\mathbf{x}_k$ having as its i^{th} component $\partial F(\mathbf{x}_k)/\partial x_{k\,i}$. Let $\mathbf{g}_k$ be an abbreviation for $\nabla F(\mathbf{x}_k)/\|\nabla F(\mathbf{x}_k)\|$, the normalized gradient evaluated at $\mathbf{x}_k$. Let $\mathbf{x}^*$ be the local minimum of $F(\mathbf{x})$ which is sought, and let $\mathbf{x}_0$ be a starting point known to be in the vicinity of $\mathbf{x}^*$.

An *ad hoc* recursive procedure to generate a sequence $\mathbf{x}_k, k = 1, \ldots$, that converges to $\mathbf{x}^*$, is given by

$$\mathbf{x}_k = \mathbf{x}_{k-1} - \alpha_k \, \mathbf{g}_{k-1},$$

where the adaptive step size α_k is computed as

$$\alpha_k = \begin{cases} 0.1 \, \|\mathbf{x}_0\| & \text{if } k = 1; \\ \alpha_{k-1}\big[0.8 + 0.5\langle \mathbf{g}_k, \mathbf{g}_{k-1} \rangle\big] & \text{otherwise.} \end{cases}$$

This procedure is similar to the method of steepest descent,[10] but differs in one important respect: instead of performing a line minimization at every step, the new point is obtained by simply stepping in the direction of the negative gradient by a small amount α_k, where the amount is determined by the recent consistency of the direction

TABLE 1: PARAMETERS AND COEFFICIENTS FOR DESIGN EXAMPLE MULTI-4-A

k	0	1	2	3
M_k	6	6	3	3
ϕ_k	0	3	1	2
$\alpha_{\omega,k}/\alpha_{n,k}$	200	200	200	200
$h_k(-18)$	-0.000231	0.000020	-0.000899	0.001515
$h_k(-17)$	-0.000079	0.000716	0.000240	-0.000981
$h_k(-16)$	0.000105	0.001570	-0.000998	-0.002864
$h_k(-15)$	0.000452	0.001785	0.000353	0.005031
$h_k(-14)$	0.003082	0.000106	0.006251	0.000710
$h_k(-13)$	0.004028	-0.004416	-0.006842	-0.007537
$h_k(-12)$	0.003071	-0.008047	-0.008776	0.005771
$h_k(-11)$	0.002914	-0.007955	0.006002	0.005817
$h_k(-10)$	-0.001578	-0.002069	-0.009996	-0.014475
$h_k(-9)$	-0.009911	-0.000532	0.007632	0.009549
$h_k(-8)$	-0.018798	-0.010125	0.038241	0.015438
$h_k(-7)$	-0.024026	-0.021252	-0.028616	-0.032447
$h_k(-6)$	-0.017681	-0.005302	-0.021791	0.011736
$h_k(-5)$	0.005064	0.053377	0.021230	0.042646
$h_k(-4)$	0.043371	0.119409	-0.100109	-0.070591
$h_k(-3)$	0.090320	0.122528	0.037468	0.007347
$h_k(-2)$	0.138675	0.022906	0.279634	0.145105
$h_k(-1)$	0.177163	-0.128418	-0.090477	-0.301496
$h_k(0)$	0.193281	-0.217235	-0.368732	0.353263
$h_k(1)$	0.181582	-0.169503	0.081644	-0.265015
$h_k(2)$	0.144921	-0.022006	0.277048	0.099983
$h_k(3)$	0.096284	0.109742	-0.028295	0.031756
$h_k(4)$	0.047843	0.141315	-0.088873	-0.065840
$h_k(5)$	0.008528	0.083225	-0.014306	0.024724
$h_k(6)$	-0.016265	0.008112	-0.033214	0.021238
$h_k(7)$	-0.026650	-0.027497	0.022877	-0.028142
$h_k(8)$	-0.021824	-0.021611	0.041910	0.006837
$h_k(9)$	-0.011048	-0.005287	-0.009335	0.011106
$h_k(10)$	-0.003766	0.000941	-0.006906	-0.013007
$h_k(11)$	0.001982	-0.004502	0.000517	0.001627
$h_k(12)$	0.004751	-0.007827	-0.009260	0.005380
$h_k(13)$	0.003698	-0.005894	0.004476	-0.005726
$h_k(14)$	0.001860	-0.000100	0.004866	0.000564
$h_k(15)$	0.000872	0.002318	-0.004093	0.001932
$h_k(16)$	-0.000163	0.001830	0.002501	-0.001037
$h_k(17)$	-0.000998	0.000358	-0.000348	-0.000272
$h_k(18)$	-0.000472	-0.000105	-0.000903	0.000323

TABLE 2: PARAMETERS AND COEFFICIENTS FOR DESIGN EXAMPLE MULTI-4-B

k	0	1	2	3
M_k	6	6	3	3
ϕ_k	0	3	1	2
$\alpha_{\omega,k}/\alpha_{n,k}$	200	200	20	2
$h_k(-18)$	-0.000045	0.000033	0.000081	0.000096
$h_k(-17)$	-0.000169	0.000686	-0.000282	-0.000161
$h_k(-16)$	-0.000574	0.001184	0.000262	-0.000223
$h_k(-15)$	-0.000375	0.001371	0.000076	0.000094
$h_k(-14)$	0.002023	-0.000092	0.000670	0.000355
$h_k(-13)$	0.004608	-0.002080	-0.000781	0.000117
$h_k(-12)$	0.005054	-0.005322	-0.000992	-0.000419
$h_k(-11)$	0.001944	-0.008161	-0.002132	-0.000714
$h_k(-10)$	-0.003749	-0.010213	0.000455	-0.000458
$h_k(-9)$	-0.009631	-0.007678	0.003272	0.000925
$h_k(-8)$	-0.019113	-0.007902	0.012255	0.001581
$h_k(-7)$	-0.025736	-0.006148	-0.006496	-0.001483
$h_k(-6)$	-0.019194	0.002672	-0.021957	0.001516
$h_k(-5)$	0.007092	0.049013	0.000655	0.002324
$h_k(-4)$	0.048219	0.104604	-0.041576	-0.023988
$h_k(-3)$	0.093235	0.121618	-0.008396	0.025608
$h_k(-2)$	0.139231	0.026922	0.290552	0.086100
$h_k(-1)$	0.177650	-0.123495	-0.077411	-0.300618
$h_k(0)$	0.194537	-0.225677	-0.411808	0.403833
$h_k(1)$	0.180053	-0.170449	0.123164	-0.259852
$h_k(2)$	0.141946	-0.014846	0.221152	0.046626
$h_k(3)$	0.093155	0.122879	0.012514	0.035721
$h_k(4)$	0.047309	0.142114	-0.056170	-0.015510
$h_k(5)$	0.009253	0.074740	-0.054574	0.000191
$h_k(6)$	-0.018000	0.001562	-0.006982	0.000415
$h_k(7)$	-0.026915	-0.025947	0.012557	-0.002910
$h_k(8)$	-0.021711	-0.016846	0.015197	0.000144
$h_k(9)$	-0.010208	-0.005945	0.003047	0.001316
$h_k(10)$	-0.002416	-0.002705	-0.002203	0.000813
$h_k(11)$	0.001528	-0.006187	-0.004353	0.000070
$h_k(12)$	0.004344	-0.005924	-0.000624	-0.000575
$h_k(13)$	0.004580	-0.004263	0.000348	-0.000590
$h_k(14)$	0.002796	-0.001050	0.001337	-0.000110
$h_k(15)$	0.000608	0.000320	-0.000091	0.000217
$h_k(16)$	-0.000327	0.000852	0.000075	0.000168
$h_k(17)$	-0.000419	0.000337	-0.000233	-0.000048
$h_k(18)$	-0.000120	0.000133	-0.000008	-0.000258

of the search (as measured by the dot product of the normalized gradient with the previous normalized gradient). The philosophy behind this strategy is simple. If the direction of the search has been consistent, as would be the case far from a local optimum, then the search is accelerated. On the other hand, if it has been inconsistent, as would be the case in the vicinity of a local minimum, then the search is decelerated. The constants 0.8 and 0.5 were empirically determined to be suitable in a large number of test cases. These constants determine the maximum and minimum possible step-size multipliers, which here are 1.3 and 0.3, respectively.

7. REFERENCES

1. M. Vetterli, "Filter Banks Allowing Perfect Reconstruction," *Signal Processing*, vol. 10, pp. 219-244, April 1986.

2. P.P. Vaidyanathan, "Theory and Design of M-Channel Maximally Decimated Quadrature Mirror Filters with Arbitrary M, Having Perfect Reconstruction Property," *IEEE Trans. on ASSP*, vol. ASSP-35, pp. 476-492, April 1987.

3. A.C. Popat, "A Note on QMf Design," MIT Advanced Television Research Program internal memorandum, MIT Media Laboratory, Cambridge, Mass., December 1988.

4. L.L. Liu, *Digital Intermediate Format for Video Frame Rate Conversion*, M.S.E.E. thesis, MIT, Cambridge, Mass., pp. 37-42, September 1990.

5. P.P. Vaidyanathan, "Quadrature Mirror Filter Banks, M-Band Extensions and Perfect Reconstruction Technique," *IEEE ASSP Magazine*, vol. 4, pp. 4-20, July 1987.

6. D. Gabor, "Theory of Communication," *J. of the IEE*, vol. 93, pp.429-457,1946.

7. J.G. Daugman, "Complete Discrete 2-D Gabor Transforms by Neural Networks for Image Analysis and Compression," *IEEE Trans. on ASSP*, vol. ASSP-36, pp. 1169-1179, 1988.

8. E.P. Simoncelli and E.H. Adelson, "Subband Transforms," in J.W. Woods, ed., *Subband Image Coding*, Kluwer Academic Publishers, Boston, pp. 143-192, 1991.

9. D. Slepian, "Prolate Spheroidal Wave Functions, Fourier Analysis and Uncertainty — V: The Discrete Case," *BSTJ*, vol. 58, pp. 1371-1430, May-June 1978.

10. D.G. Luenberger, *Linear and Nonlinear Programming*, Addison-Wesley, Reading, Mass., 1984.